

Soft Physics, Centrality and Multiplicity at RHIC

D. E. Kahana, S. H. Kahana

*Physics Department, Brookhaven National Laboratory
Upton, NY 11973, USA*
(December 5, 2018)

The inclusive spectra so far accumulated at the Relativistic Heavy Ion Collider (RHIC) at energies of $\sqrt{s} = 56, 130$ and 200 GeV are examined within the hadronic simulation LUCIFER. What emerges at this juncture is a comprehensive and clear picture of soft physics which apparently dominates the intermediate and later stages of the ion collisions. The focus is on energy and centrality dependence of the mid-rapidity charged spectra, using an analysis based for the most part on production and rescattering of intermediate generic resonances. The bosonic, ρ - and K^* -like resonances, produced in initial nucleon-nucleon interactions and materialising only after some delay time, behave as an incompressible fluid with saturated number and energy density.

25.75, 24.10.Lx, 25.70.Pq

I. INTRODUCTION

A possible conclusion to be drawn from initial observations of inclusive charged particle spectra in Au + Au collisions at RHIC, by the four detectors PHOBOS [1], PHENIX [3], BRAHMS [4] and STAR [5], which observations, of course, are only of the final state of the collision, is that soft, strongly interacting QCD plays a dominant role in the dynamics. To be sure, there do exist potentially interesting anomalies in high p_\perp charged [6] and neutral [7] pion spectra, among others. These occur for p_\perp in the range 2–4 GeV/c, involve only a small fraction of the integrated cross-section, and may in fact be describable by an energy loss mechanism for π mesons acting in the later stages of a collision.

The hadronic simulation LUCIFER [8–10] has already given a good description [10] of the earliest PHOBOS [1] and STAR [5] measurements of averaged mid-rapidity cross-sections for charged particles, $(dN/d\eta)^{ch}$ for $|\eta| \leq 1$, including also a successful prediction [9,11] of the surprisingly slight (10–14%) rise in this observable as the collision energy is increased from $\sqrt{s} = 130$ GeV to 200 GeV. Also correctly anticipated was the shape of the pseudo-rapidity spectrum for charged particles at higher values of η [10–12].

Here, we consider simulation results for the centrality dependence which is found by all of the detectors [5,7,12,14]. These collaborations emphasize the variation of $(dN/d\eta)^{ch}|_{\eta=0}$ with the number of participants. This work concerns itself with comparisons of the spectral magnitudes and shapes as a function of centrality. The variation of experimentally defined centrality is directly related theoretically to changes in the impact parameter b . The energy and geometrical dependence extracted from LUCIFER speak directly to assumptions underlying the cascade simulation, and to the nature and the number density of the resonance rescatterers employed in the model.

In earlier work [8–10] we stressed that the role of our simulation was only to define the ‘ordinary,’ giving experimentalists a background calculation against which to judge potentially unusual data. There do, of course, exist a variety of other simulations [15–20,22–24], having similar goals but differing approaches: some are purely partonic models and some are hybrid partonic-hadronic.

It seems again appropriate to compare the, by now, extensive observations at RHIC with simulations which do not assume that plasma is necessarily present. The purest such comparison would employ a model involving only colour singlet, hadronic degrees of freedom. The physical picture is one in which ion-ion collisions are describable in the main by multiple interactions between excited hadrons only. In such a picture, constituent quarks, present within original and produced baryons, are perhaps raised to states differing from those present in the lowest mass baryons, but glue holding the valence quarks in place remains ‘sticky.’ So quarks and gluons continue to act as if still confined within hadrons. In addition to excited baryons, color singlet bosonic degrees of freedom are produced and play a significant role. Such a description has proven feasible in the Pb + Pb collisions examined in NA49 [25,26]. In fact, excited bosons only enter at a later stage of the simulation, often after some initial baryon-baryon interactions are completed. It remains to be seen whether at the higher energies of RHIC a large number of partons, carrying a large fraction of the energy density, perhaps ‘minijets’ [27], are in fact free and able to roam over large spatial distances, and more importantly whether sufficient ‘free’ gluons are present to create the thermodynamic basis for material which could be described as quark-gluon plasma.

The simulation we employ has two successive stages. In phase I, no energy is removed for soft processes. Therefore, initial baryon-baryon interactions take place very nearly on the light cone. The construction of a collision history

is guided by inputs from NN data, the key ones being: (1) absolute total cross-sections as a function of energy, (2) branching ratios for elastic and various inelastic processes and (3) multiplicity distributions for meson production.

Our two body model has been discussed extensively in earlier work [9,10]. It attempts to emulate multi-peripheral models of nucleon-nucleon scattering which divide the total cross-section into elastic, single diffractive and non-single diffractive [28] processes. Our assumption is that generic ρ -like and K^* -like resonances are the major rescatterers, *only entering into phase II*, of the simulation, which begins after a formation time τ_f , a central model parameter, has elapsed for particles produced in phase I, in their various rest frames. Since these resonances themselves decay into multiple particles stable under the strong interaction on a time scale τ_d , which is a second important model parameter, their multiplicities must be adjusted appropriately so as to reproduce free space NN data, and they are in fact reduced in number by some two to three times relative to the expected multiplicity of stable mesons. Importantly however, it then follows that any model reproducing the known nucleon-nucleon data, such as explicit string models [16,18], could have been employed up to the commencement of phase II of the simulation.

We use a resonance model of nucleon-nucleon scattering for reasons which will become clear as we proceed and because interactions which are particle-like in nature are easier to deal with than, say, the interactions of strings. We will discuss the spatial and energy densities of the ‘rescatterers’ at some length in what follows and thus make evident a simplicity in both the energy and centrality dependence of the observed pseudo-rapidity densities which arises from such considerations. It appears that over an appreciable range of both energy and impact parameter, the density of generic hadronic resonances, built up during phase I, must remain nearly constant in ion-ion collisions, if the observed centrality and energy dependence of final charged particle spectra are to be correctly described. The extracted resonance size, assuming close packing or saturation, is eminently reasonable.

We again adopt the position that the analysis for Au + Au at RHIC simply presents an extrapolation from earlier NA49 inclusive measurements [10,25,26] to the considerably higher energy RHIC collisions. We could equally well have normalized the absolute level of meson production to the lowest RHIC energy ($\sqrt{s} = 56$ GeV). This normalization directly implies a determination of the average density of generic resonances, or rescatterers, in phase II of the LUCIFER simulation for Au + Au, a theoretical observable which is then a single number characterising presently measured inclusive RHIC physics.

Uniformity in resonance production is achieved by imposing an upper limit on total multiplicity in contiguous groups of interacting nucleons within an A + A event [9,10] or, equivalently, by imposing a limit directly on the two body interactions themselves. This is accomplished by introducing this limit at a single energy. The density of the saturated resonance fluid is fixed by normalising the simulated multiplicity to the experimental multiplicity at a fixed total energy in a massive (large A) ion-ion collision. No such restriction is imposed on pure NN interactions, or for example p + D collisions. Previously, [8,9] we based our approach on ideas put forward by Gottfried [29] in describing p + A collisions. Gottfried delayed interactions of particles produced in the successive NN interactions in a p + A collision, until the produced particles were physically sufficiently separated from each other and their progenitors to act as separate hadrons. The extra constraint which we impose, saturation of the rescatterer density in ion-ion collisions, may be occasioned when multiple resonances produced in neighbouring NN collisions interfere with one-another. It is almost self evident that individual resonances condensing from such two body collisions cannot overlap.

After a short digression on the details of LUCIFER, we develop the above ideas in two ensuing sections. First, comparisons are presented between the model and the experimental results at RHIC from the various detectors, large and small. These include charged particle pseudo-rapidity measurements at $\eta = 0$ for varying centrality, at the first RHIC energy $\sqrt{s} = 130$ GeV analysed in this fashion. Also treated is the energy dependence for $(dN/d\eta)^{ch}|_{\eta=0}$ at $\sqrt{s} = 56$, 130, and 200 GeV, using for the lowest energy, data which are available only from the PHOBOS [1] collaboration. Also considered at $\sqrt{s} = 130$ GeV, are the full pseudo-rapidity distributions for differing degrees of centrality.

Secondly, the distributions of underlying rescatterers, *i. e.* the dependence of the number of boson-like resonances, $N_{RES}(b, s)$, on impact parameter and energy, are extracted from the simulations. The simple relations for the spatial and energy distributions thus obtained illuminate the physical basis for the overall simulation. In particular, the number density of meson resonances reached at the formation time τ_f , although not large, is sufficient to explain the observed stable meson production. The baryon density from the onset of an AA event up to the earliest formation time $t=\tau_f$, involves far fewer particles, but could still in principle provide problems. The latter will be discussed at an appropriate point.

II. LUCIFER: DYNAMICS AND INPUTS

For completeness we present a brief outline of the dynamics in LUCIFER [9,10]. Phase I has been adequately described above and sets the initial conditions for an ordinary hadronic cascade (with energy loss) in phase II [21,22,24]. The numbers and the properties (flavour, mass, *etc.*) of hadrons entering into phase II are determined in phase I by recording all baryon-baryon collisions. Providing complete initial conditions for phase II requires us to specify four momenta and positions for the produced resonances. The positions are simply randomly distributed along the paths of nucleons colliding in phase I, while the momenta must conserve overall energy and momentum and be consistent with production and phase space in NN collisions. Existing baryons acquire transverse momentum by making a random walk in the number of collisions, and softly produced meson resonances are given transverse momenta commensurate with soft production as observed in NN collisions. The total multiplicity of the resonances is restricted as described above. We reemphasise that the generic resonances first appear only in phase II. The latter is a normal cascade in which energy is lost at each binary collision and during which the resonances both interact with each other and decay into pions and other stable particles. The restricted range of masses for the resonances, 300-1200 MeV, or somewhat higher if strangeness is involved, guarantees we have only soft processes, *i. e.* that only relatively low p_\perp is generated in the decays.

We have listed the important two-body inputs in phase I, but we should make more explicit a very important feature in the elementary model, *viz* the energy dependence of the multiplicity distributions, which obey KNO-scaling [31]. Our description of the scaling of the multiplicity distributions comes from fitting multi-prong data mostly drawn from the UA(5) experiment [30]. Central to this parameterization is the energy dependent average number of prongs $\bar{n}(s)$ entering through the definition of KNO scaling

$$n = \bar{n}(s) f\left(\frac{n}{\bar{n}(s)}\right). \quad (1)$$

Although we artificially limit the number of mesons produced in ion-ion collisions by our no-overlap constraint on the generic resonances, the energy dependence for increasing production of these particles still drives the final multiplicities as a function of s . In Figure 1 we display a *De facto* prediction of the two body model, *i. e.* which arises via the energy dependence of $\bar{n}(s)$. This is the comparison of calculated energy variation of central charged multiplicity, $(dN/d\eta)^{ch}(s)|_{\eta=0}$ with data [32-34]. Since one is here dealing with a collision involving two incoming nucleons (participants) this quantity is, in effect, already divided by 1/2 times the number of participants. The slight increase predicted for the rise in $(dN/d\eta)^{ch}|_{\eta=0}$ for Au + Au, going from $\sqrt{s} = 130$ GeV to 200 GeV, arises essentially completely from the energy dependence of \bar{n} : this dependence is weak in the two body data and equally weak for ion-ion collisions. This is a dynamic, and not merely kinematic, outcome of the simulation, but it is one which follows from the NN character of phase I.

III. CENTRALITY DEPENDENCE OF RAPIDITY DISTRIBUTIONS: LUCIFER VS DATA.

Figure 2 reviews earlier $(dN/d\eta)^{ch}|_{\eta=0}$ results for the most central collisions, indicating the predicted 12-14% rise between $\sqrt{s} = 130$ and 200 GeV for Au + Au at RHIC [10,11]. A more complete picture of the variation in this pseudo-rapidity density $(dN/d\eta)^{ch}|_{\eta=0}$ for varying centrality cuts is shown in Figure 3 with LUCIFER compared to the existing detector data [3,5,11,12] for the 130 GeV runs. The centrality cuts on the simulation are defined in terms of the calculated dN/db , which is integrated to give the appropriate degree of centrality between limits b_1 and b_2 , $\Delta b = b_2 - b_1$. Theoretical curves describing this b dependence are shown in Figure 4. A more expeditious definition of the percentage centrality was employed earlier [10]. This convenient geometrical definition is not necessarily in accord with actual experimental usage. The agreement between simulation and measurement persists out to rather high impact parameter, possibly deteriorating somewhat for $b \geq 8$ fm. For peripheral collisions the ‘constancy’ of resonance density, discussed in detail below, is not maintained in our saturated simulations. Indeed for the most peripheral collisions, with say only a few nucleons colliding, there should be no multiplicity suppression.

One should also confront the full pseudo-rapidity distributions insofar as they have been measured; this we do in Figure 5 using PHOBOS data at $\sqrt{s} = 130$ GeV [11]. The higher energy $\sqrt{s} = 200$ yields similar comparisons. Again the agreement in shape is seen to be adequate. So the most inclusive meson data, taken at $\sqrt{s} = 130$ GeV, is well described by the present two phase cascade. Finally, to demonstrate the similarity with other presentations of the data we include a plot, Figure 6, of participant nucleon number, $N^{part}(inelastic)$, in LUCIFER versus the ‘number of participants’ which was abstracted from two of the experiments. In the simulation we can easily estimate the total $N^{part}(inelastic)$ by counting the number of spectator nucleons (they are just those initial nucleons which had no inelastic collisions in phase I or II of the cascade) in a sample of events having some fixed b and subtracting

that number from the total number of initial nucleons. Of course only inelastic participants, which contribute to the multiplicity, must be selected for comparison with experiment where the distinction between ‘inelastic’ participants and ‘elastic’ participants becomes moot, so that another subtraction of purely elastic participants must be made theoretically. For the degree of centrality reached in the experiments, $\leq 50\%$, this additional adjustment is small, but it would become an appreciable correction, tending to $\sim 20\%$, in more peripheral events.

IV. RESONANCE MULTIPLICITY DEPENDENCES ON B AND \sqrt{S}

A. Fire Cylinder and Transverse Areal Density

Most of the simulation results can be understood in terms of simply constructed model quantities. At the commencement of the ‘soft’ cascade, phase II, we constrained the system to avoid spatial overlap of the rescatterers. The extent to which this succeeds can be quantified as a function of impact parameter. Plotted in Figure 7 is the distribution of the ρ -like resonances as a function of b , at the start of phase II. There is of course a dispersion in the numbers $N_{RES}(b, s)$, reflecting fluctuations from event to event, but a good estimate of the areal density of resonances can still be made. We use the term ‘areal’ density in referring to the number of resonances in the area of overlap of the two nuclei, obtained when the overlap volume from phase I is projected into a plane transverse to the beam direction, for fixed impact parameter.

The overlap volume or interaction region has, in our simulation of a gold-gold collision, for early times $t > \tau_f$ very nearly the form of a generalised cylinder. The directrix of this cylinder is a convex curve formed by the two circular arcs bounding the projection of the overlap volume of the spherical nuclei into the transverse plane. The generator of the cylinder is parallel to the beam direction and along the direction of longitudinal expansion of the interaction region. Perhaps this volume could be appropriately be termed a ‘fire cylinder.’ The area in question then, is the transverse cross-section of the fire cylinder. Taking the geometry of the two colliding nuclei to be sharply spherical, with radius R , the area of overlap $A(b)$ can be calculated:

$$A(b) = 2R^2 \left[\cos^{-1} \left(\frac{b}{2R} \right) - \left(\frac{b}{2R} \right) \sqrt{1 - \left(\frac{b}{2R} \right)^2} \right]. \quad (2)$$

For $b \leq R$, the areal density of resonances is then found to be:

$$\sigma_a(b, s) = N_{RES}(b, s)/A(b). \quad (3)$$

Sample curves obtained for this density are exhibited in Figure 8 for varying choices of nuclear radius $R = 6.8, 7.0, 7.2$ fm, the latter value being closer to the actual situation for gold nuclei, especially when the addition of a surface diffusivity converts the nuclear geometries into the more realistic forms we employ in the Monte-Carlo. This figure demonstrates, however, the near constancy of $\sigma_a(b)$ out to rather large separations of the colliding nuclei, $b \sim 8-10$ fm. This perhaps surprisingly accurate, but intuitively satisfying, uniformity of the resonance population of the fire cylinder is a representation of the constraints placed on production. The result of imposing constancy strictly out to $b = 10$ fm is included in the above Figure 3. Measurements seem to be telling us that indeed the transverse density $\sigma_a(b, s)$ varies very little.

A reasonable approach for still more peripheral events would be to smoothly cut off the degree of suppression of the resonance multiplicity, until for the most glancing collisions there was no multiplicity suppression at all, at which point one expects after all that only unadulterated two body reactions occur. The results for the latter eventuality are shown in Figure 1, as explained previously a prediction of the elementary two-body model used here and extracted, in fact, from p+D reactions.

B. Fire Cylinder Volume and Energy Dependency

It is more difficult to precisely define a volume for the interaction region or fire cylinder at the onset of phase II of the simulation, the soft cascade. From figure 9 it is clear that after time $t = \tau_f$ in the center of momentum (lab) frame, up to the time of termination of phase II, new resonances are continually appearing, at times related to their velocities β_i via $t_i = \gamma_i \tau_f$, γ_i being the Lorentz factor peculiar to the i ’th resonance. In the final analysis, a choice $\tau_f = 1.2 - 1.6$ fm/c for the formation time was made, with globally similar results. In general, it is clear there is some interplay between τ_f and the overall normalisation of resonance number. A more extended delay time implies a more

expanded system and less cascading in phase II. Too short a formation time could in fact lead to an inability for the simulation to keep within the experimental limits for total meson numbers. No such problem arises for the range of τ_f selected above, and these total numbers as a function of centrality are well reproduced.

For these last issues of spatial densities we choose the most central collisions with $b \leq 4$, although little would be changed by using a fixed impact parameter. Figure 10 demonstrates the strong interdependence between the number of resonances $N_{RES}(s)$ and the average longitudinal Lorentz factor $\bar{\gamma}_z(s)$ (the averaging here is over all resonances). $\bar{\gamma}_z$ is directly related to the average length of the fire cylinder in the longitudinal direction:

$$L_z(s) = 2\tau_f \bar{\gamma}_z. \quad (4)$$

The energy dependence of $N_{RES}(s)$ is then very simply and naturally described in Figure 10, and is another dynamical statement of the model. The cylinder length grows linearly with $\bar{\gamma}_z$ for increasing s , once again a useful and easily understood, result.

It is then an easy matter to compute the volume of the fire cylinder

$$V(b) = A(b)L_z(s), \quad (5)$$

and thus to obtain the three dimensional number density:

$$\rho(b, s) = \sigma_a(s)/L_z(s). \quad (6)$$

For this selection of very central collisions $\rho(s)$ is found to be $\sim 0.70 - 1.10$ particles per fm^3 , depending on the specific choices for nuclear radius and τ_f in Figure 8. This leads to an average resonance size of ~ 0.70 fm. Of course, in the simulation we treat the generic scatterers as points and their extracted size is simply a statement of the volume each resonance occupies, more or less at the time it is created. It is, however, significant that such a size is eminently reasonable for a hadronic resonance, and that the associated number density is consequently relatively low. These averages obtain of course after the formation time τ_f in the rest frame of produced mesons, but considerably later in say the c. of m. Nevertheless, to use an earlier, ‘average’ time would also involve less produced particles, and the fire cylinder densities we introduce would be little influenced.

V. TRANSVERSE NUMBER AND ENERGY DENSITIES

One can also estimate the transverse energy densities, $\rho_\epsilon(t)$, associated with the above number density $\rho(b, s)$. Considering, for now, only the dominant bosonic contribution, one arrives at a total $\sim \sqrt{(1)^2 + (1)^2}$ GeV *i. e.* ~ 1.4 GeV/ fm^3 . This since the average bosonic mass is somewhat over 1 GeV and its average p_\perp in phase I is somewhat under 1 GeV/c. To this must be added the energy density from baryons present at the initiation of phase II, an increase within the fire cylinder imagined above of some 20%; thus overall $\rho_\epsilon(t) \sim 1.7$ GeV/ fm^3 . The density $\rho_\epsilon(t)$ is an average over many events constructed at the start of phase II, and is well below the average Bjorken value quoted by the RHIC experimental collaborations. Almost independent of collider energy, a major proportion, some 40% of the final mesons, and hence also a large fraction of the transverse energy, is produced via the collisions taking place in phase II [10] of the simulation. The variation in this fraction is only a few percent from 56 to 200 GeV/A. Combining the contributions from I and II would yield ~ 2.8 GeV fm^3 , still short of the Bjorken estimate. Part of this discrepancy in total transverse energy densities is explained by our use of a longer formation time. However, since the final phase of the cascade occurs when the system has surely expanded considerably spatially, the extra transverse energy generated in II contributes little to the early density, often used as a trip wire in theoretical models for the initiation of ‘plasma’ creation.

The question of detailed double differential cross-sections, $d^2N/d\eta p_\perp dp_\perp$, especially those at the highest transverse momenta measured, will be examined thoroughly in ensuing work. For now we present in Figure 11 a preliminary comparison between STAR data [6] and LUCIFER, pertaining to total negative hadron (h^-) production below $p_\perp = 4\text{GeV}/c$. The higher ranges of this comparison, say $p_\perp \geq 2$ GeV, are possibly beyond the limits of our current modeling which largely omitted hard processes in the underlying two body scattering. Large p_\perp events certainly require more study, but the present results are nevertheless interesting. The highest p_\perp particles are produced in the simulation by multiple scattering and are thus subject to normal energy losses expected in such scattering. Despite this reservation, the rapid drop in $d^2N/d\eta p_\perp dp_\perp$ assures one that the softer part of the spectrum dominates total transverse energy production. Thus the total transverse energy E_t generated in the cascade is close to that seen experimentally.

Of course we cannot really say what transpires in the earliest stages of the ion collision. We have made certain assumptions about hadron tenacity and saturation and have then obtained at the close of the second stage of the cascade conditions very much like those observed for the global, inclusive, production processes. One problem,

mentioned in the Introduction, concerns the earliest phase of the collision, perhaps even before the production of bosonic resonances, and involves the purely baryonic densities. If one assumes each nucleus is never less than 1 fm in transverse extent, then for $b = 4$ fm collisions the baryon density does not rise much above one per fm³.

Further, the successful use of generic resonances to describe the cascading might simply reflect a correct fixing of average cross-sections and cross-section ‘flow’ during an ion-ion event.

VI. COMMENTS AND CONCLUSIONS.

The two phases of the LUCIFER simulation have been merged into a single, idealized, dynamical model. Such a model can be only a part of the complete story, of course; partonic degrees of freedom do exist and for sufficiently high particle transverse momentum presumably will dominate the inclusive spectra. Nevertheless, in our approach centrality and energy dependence comparisons between data and simulation are understood as arising from a common physical origin: the uniform and unvarying density of resonances in the fire cylinder. The constancy of areal and volume densities of bosonic resonances and their close to linear dependence in energy with \sqrt{z} are notable results of the simulation.

The dynamics of the collision is split into two phases, sequential in time: one could have created the initial conditions for phase II in some alternate fashion, for example by attributing the initial meson distributions to a string model or to de-confinement and hadronisation of partons [18,35]. Our sole and central point here is, then, that signals other than those so far observed should show up to distinguish the present cascade from such alternatives, especially from nearly complete parton de-confinement. The string approach may in fact lead to the same results in simulating a massive ion-ion collision. We reiterate that the two-body modeling and cascading in phase I leaves strong footprints in the final results, especially in the surprisingly gentle increase in predicted, and measured, $(dN/d\eta)^{ch}|_{\eta=0}$ seen from $\sqrt{s} = 130$ to 200 GeV.

No one can doubt that there is a saturation effect observed in meson production at RHIC. To produce this effect, we reduce cascading in two fashions: (1) through the very presence of the boson resonances which eventually decay, over both phases I and II, into many more π or K mesons ($\sim 4\text{--}5$), and (2) through the near constant resonance density in the fire cylinder achieved in central collisions. This latter can be imposed in principle via, and is equivalent to, placing a no spatial overlap constraint on the produced resonances prior to the soft cascade. The data, Figure 3, suggest a more strict uniformity than produced in the cascade.

In any case, the relatively small observed total multiplicities, which present a problem for all models, do not strongly support a large increase in the number of degrees of freedom in the early phase of Au + Au collisions at RHIC.

One should add that no attempt was made here to divide the output of the cascade into separate dependences on numbers of participants or on the numbers of binary collisions. The cascade does this dynamically and seamlessly. One might note, however, that the participant number directly determines the overall incoming energy put into an ion collision in phase I and thus also fixes the number of resonances at reinitialisation and commencement of phase II. The division into two phases does, however, distinguish the present approach from some alternatives; principally in reducing the generation of transverse energy at very early times.

We will return in later work to more specific questions, *e. g.* of flavour generation and high transverse momentum spectra, but we mention here that close to the correct ratios of strange meson production at mid rapidity, are obtained in the calculations. These contribute some 10% of the particle number there.

This work addresses only gross, inclusive features of existing RHIC data. Accordingly, the results only suggest that non-standard medium effects must be looked for in more exclusive, rare events, whose analysis we all await. Places to look might include still higher transverse momenta spectra, direct γ -rays, $\mu^+\mu^-$ and e^+e^- pairs, or possibly just a sampling of events containing unusually high multiplicity fluctuations.

VII. ACKNOWLEDGEMENTS

This manuscript has been authored under the US DOE grant NO. DE-AC02-98CH10886. One of the authors (SHK) is also grateful to the Alexander von Humboldt Foundation, Bonn, Germany and the Max-Planck Institute for Nuclear Physics, Heidelberg for continued support and hospitality. Useful discussion with the BRAHMS, PHENIX, PHOBOS and STAR collaborations are gratefully acknowledged.

[1] B. Back et al., the PHOBOS Collaboration, *hep-ex/0007036*; B. Back et al., *Phys. Rev.Lett.* **85**, 3100,(2000).

[2] I. G. Bearden et al, BRAHMS Collaboration, *Phys. Lett.* **B523**, 277 (2001).

[3] K. Adcox et al., PHENIX Collaboration, *Phys. Rev.Lett.* **86**, 3500 (2001).

[4] I. G. Bearden et al, BRAHMS Collaboration, *Phys. Lett.* **B523**, 277 (2001).

[5] C. Adler et al, STAR Collaboration, *Phys. Rev.Lett.* **87**, 112303 (2001).

[6] C. Adler et al, STAR Collaboration, *nucl-ex/026011*.

[7] K. Adcox et al., PHENIX Collaboration, *Phys. Rev.Lett.* **88**, 022301(2002).

[8] D. E. Kahana, *Proceedings, RHIC Summer Study'96*,175-192, BNL, July 8-19, 1996.

[9] D. E. Kahana and S. H. Kahana, *Phys. Rev.* **C58**,3574 (1998); *Phys. Rev.* **C59**,1651 (1999).

[10] D. E. Kahana, S. H. Kahana, *Phys. Rev.* **C63**, 031901(2001); Proc. International Conference on the Physics of the Quark-Gluon Plasma, Ecole Polytechnique, Palaiseau, France, Sept. 4-7, 2001.

[11] M. Baker for the PHOBOS Collaboration, Proceedings of the International Workshop on the Physics of the Quark-Gluon Plasma, Paris, France, Sept. 4-7, 2001; to appear in Les Editions de l'Ecole Polytechnique.

[12] F. Videbaek for the BRAHMS Collaboration, *Nucl. Phys.* **A698**, 29c-38c (20002)

[13] K. Adcox et al., PHENIX Collaboration, *Phys. Rev.Lett.* **88**, 242301,(2002).

[14] B. Back et al., PHOBOS Collaboration, *Phys. Rev.* **C65**, 31901R,(2002).

[15] X. -N. Wang and M. Gyulassy, *Phys. Rev.* **D44**, 3501 (1991); *nucl-th/000814*

[16] B. Andersson, G. Gustafson, G. Ingleman, and T. Sjostrand, *Phys. Rep* **97**, 31 (1983); B. Andersson, G. Gustafson, and B. Nilsson-Almqvist, *Nucl. Phys* **B281**, 289 (1987)

[17] J. Ranft and S. Ritter, *Z. Phys.* **C27**, 413 (1985); J. Ranft *Nucl. Phys.* **A498**, 111c (1989); A. Capella and J. Tran Van, *Phys. Lett.* **93B**, 146 (1980) and *Nucl. Phys.* **A461**, 501c (1987):

[18] K. Werner, *Z. Phys. C* **42**, 85 (1989); K. Werner, J. Aichelin, *Phys.Rev.Lett.* 76 (1996) 1027-1030; H. J. Drescher, M. Hladik, S. Ostapchenko, K. Werner, Proc. of the "Workshop on Nuclear Matter in Different Phases and Transitions", Les Houches, France, March 31 - April 10, 1998.

[19] D. Boal, *Proceedings of the RHIC Workshop I*, (1985) and *Phys. Rev.* **C33**,2206 (1986); K. J. Eskola, K. Kajantie and J. Lindfors, *Nucl. Phys.* **B323**, 37 (1989);

[20] K. Geiger and B. Mueller *Nucl. Phys.* **B369**, 600 (1992); K. Geiger *Phys. Rev.* **D46**, 4965, and 4986 (1992). K. Geiger, *Proceedings of Quark Matter'83*,*Nucl. Phys.* **A418**, 257c (1984); K. Geiger, *Phys. Rev.* **D51**, 2345 (1995)

[21] Y. Pang, T. J. Schlagel, and S. H. Kahana, *et al*, *Phys. Rev. Lett* **68**, 2743 (1992); S. H. Kahana, D. E. Kahana, Y. Pang, and T. J. Schlagel, *Annual Reviews Of Nuclear and Particle Science*, **46**, 1996, (ed C. Quigg)

[22] H. Stoecker and W. Greiner, *Phys. Rep.* **137**, 277 (1986); R. Mattiello, A. Jahns, H. Sorge and W. Greiner, *Phys. Rev. Lett.* **74** 2180, 1995

[23] H. Stoecker, *Proceedings, RHIC Summer Study'96 and references therein*.

[24] B. Zhang, C. M. Ko, B-A, Li, Z. Lin, *nucl-th/9904075*.

[25] T. Wienold and the NA49 Collaboration; In Proceedings of Quark Matter '96, *Nucl. Phys.* **A610**, 76c-87c, 1996; P. G. Jones and the NA49 Collaboration; In Proceedings of Quark Matter '96, *Nucl. Phys.* **A610**, 76c-87c, 1996;

[26] H. Appleshauser et al. *Phys. Rev.Lett.* **82**, 2471, 1999.

[27] K. Eskola, *Proceedings, RHIC Summer Study'96*, 99-110, BNL, July 8-19,1996

[28] k. Goulian, *Phys. Rep.* **101**, 169 (1983)

[29] K. Gottfried, *Phys. Rev. Lett.* **32**, 957 (1974); and *Acta. Phys. Pol* **B3**, 769 (1972)

[30] G. Ekspong for the UA5 Collaboration, *Nucl. Phys.* **A461**, 145c (1987); G. J. Alner for the UA5 Collaboration, *Nucl. Phys.* **B291**, 445 (1987).

[31] Z. Koba, H. B. Nielsen, and P. Olesen, *Nucl. Phys.* **B40**,317 (1972).

[32] G. Alner et al., *Z. Phys.C* **33**,1 (1986); K. Alpgard et al., *Phys. Lett.* **B115**, 71,(1982).

[33] F. Abe et al., *Phys. Rev.* **D41** 2330, (1990).

[34] C. Albajar et al., *Nucl. Phys.* **B335**, 263 (1990);

[35] D. Kharzeev, E. Levin, *Phys. Lett.* **B523**, 79-87 (2001) ; J. Schaffner-Bielich, D. Kharzeev, L. McLerran and R. Venugopalan, *Nucl. Phys.* **A705**, 494-507, (2002).

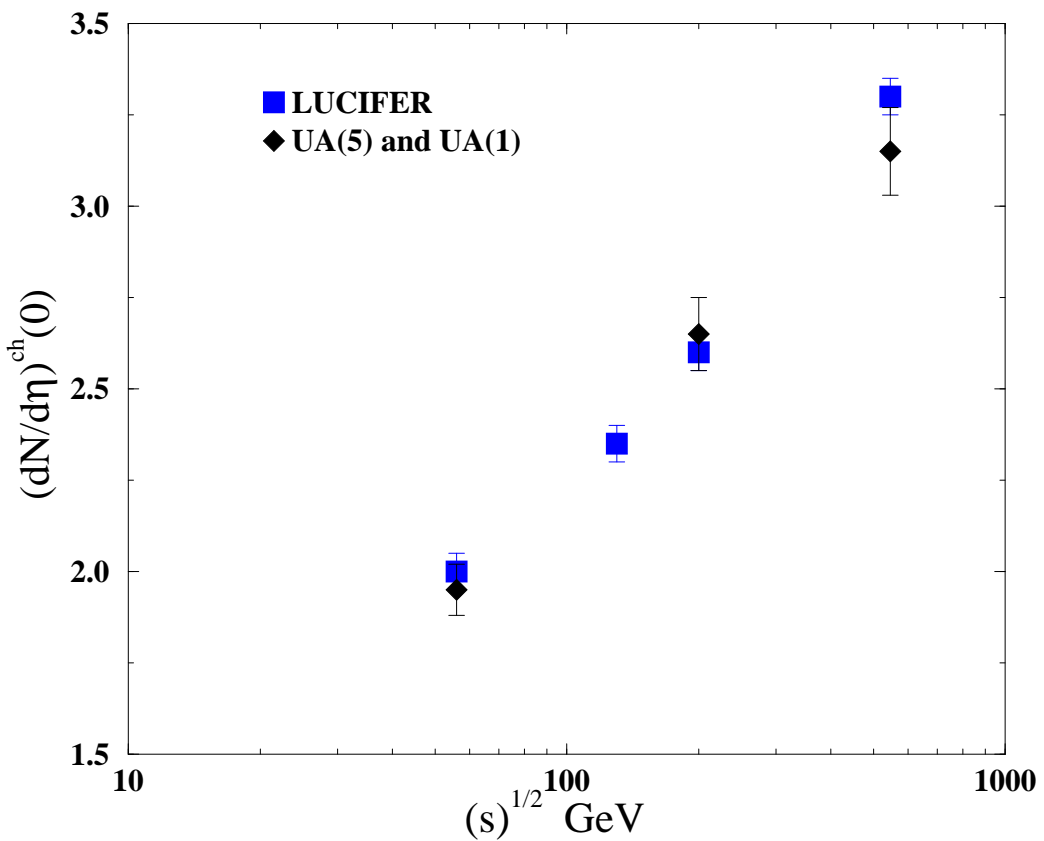


FIG. 1. Proton/Anti-proton charged meson densities for $\eta = 0$ at energies relevant to RHIC vs those extracted in $p + D$ from LUCIFER. The agreement with elementary measurements from UA(5) and UA(1) displayed is in fact a prediction of the two body model used in LUCIFER, since the basic inputs are the multiplicity distributions from single and non-single diffractive data and hence also the average multiplicity $\bar{n}(s)$ in the KNO distributions assumed.

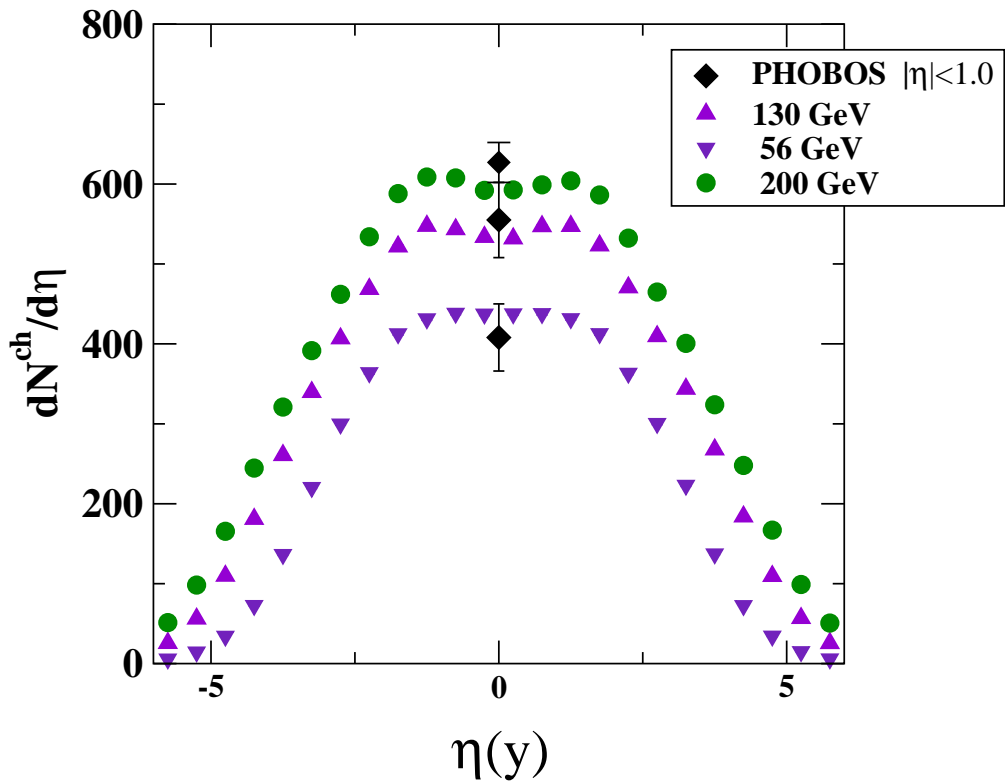


FIG. 2. Previously obtained comparison with PHOBOS $\sqrt{s} = 56$ and 130 GeV $dN^{ch}/d\eta|_{\eta=0}$ indicating what was then a prediction for the as yet unmeasured 200 GeV run. The latter data now exists. The small relative rise from 130 to 200 GeV in the $|\eta| < 1$ point is a prediction of the model.

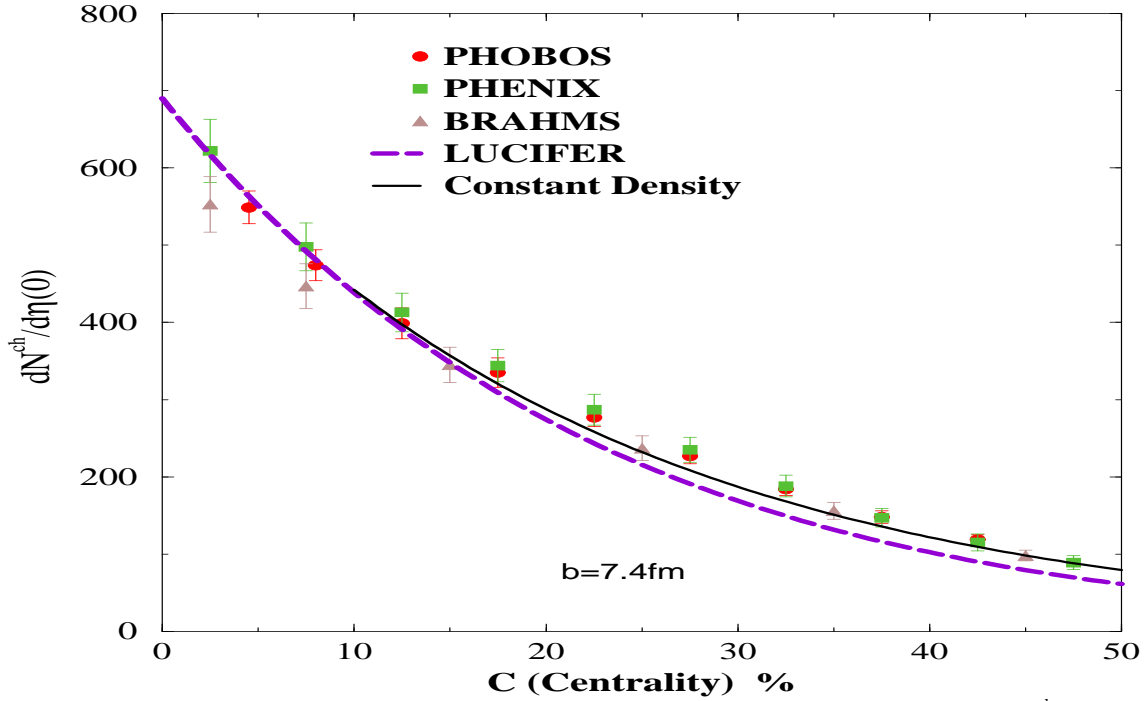


FIG. 3. Comparison with $\sqrt{s} = 130$ GeV data from three of the RHIC experiments for $(dN^{ch}/d\eta)(\eta)$ as a function of the degree of centrality. The latter is defined through the percentage of total cross-section measured, experimentally, and in the simulation by a similar quantity determined geometrically from the impact parameter range Δb spanned. The dashed line is a fit in the form $dN^{ch}/d\eta = 690 \exp\{-0.0445C - 0.00008C^2\}$. The upper solid curve indicates the result obtained if the transverse areal density, defined in Eqn. (3) and displayed in Fig.8, is held constant.

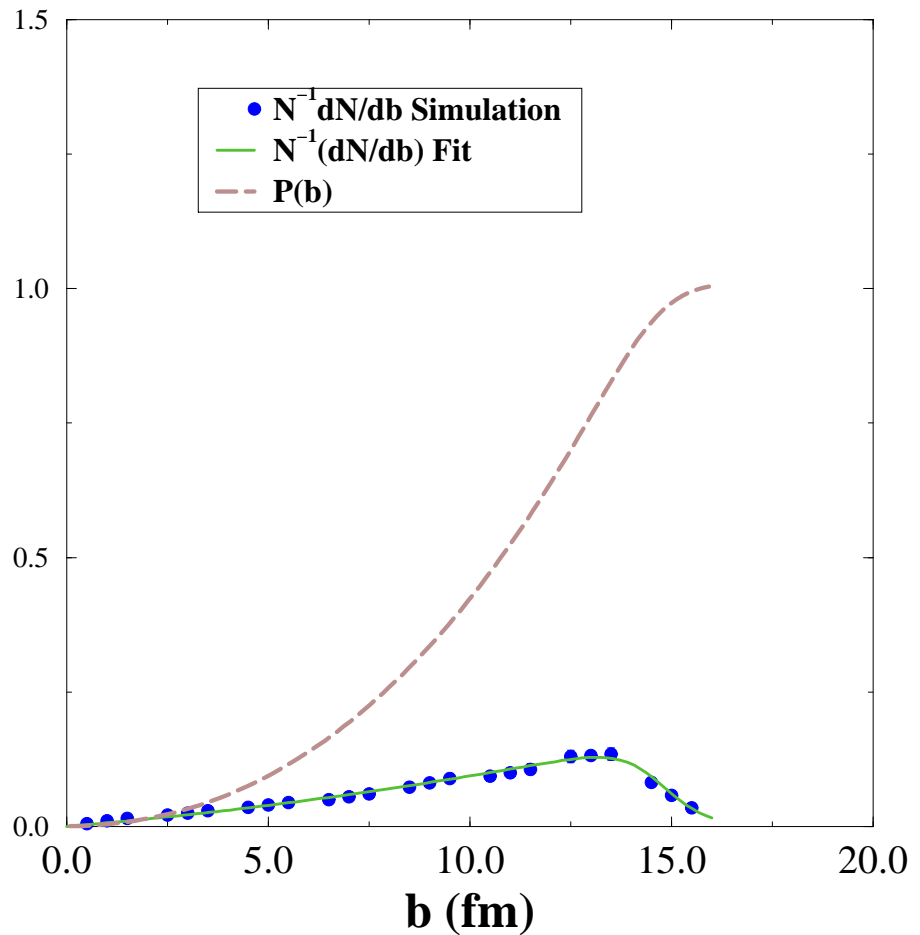


FIG. 4. Centrality vs Impact parameter in LUCIFER at $\sqrt{s} = 130$ GeV. The lower curve is a fit to the simulation data points in the form $N^{-1}dN/db = \frac{1}{160}[b + .05b^2]/[1 + \exp\{1.8(b - 14.6)\}]$ while the upper curve, giving the probability distribution $P(b)$ of centrality vs b , is obtained by integration.

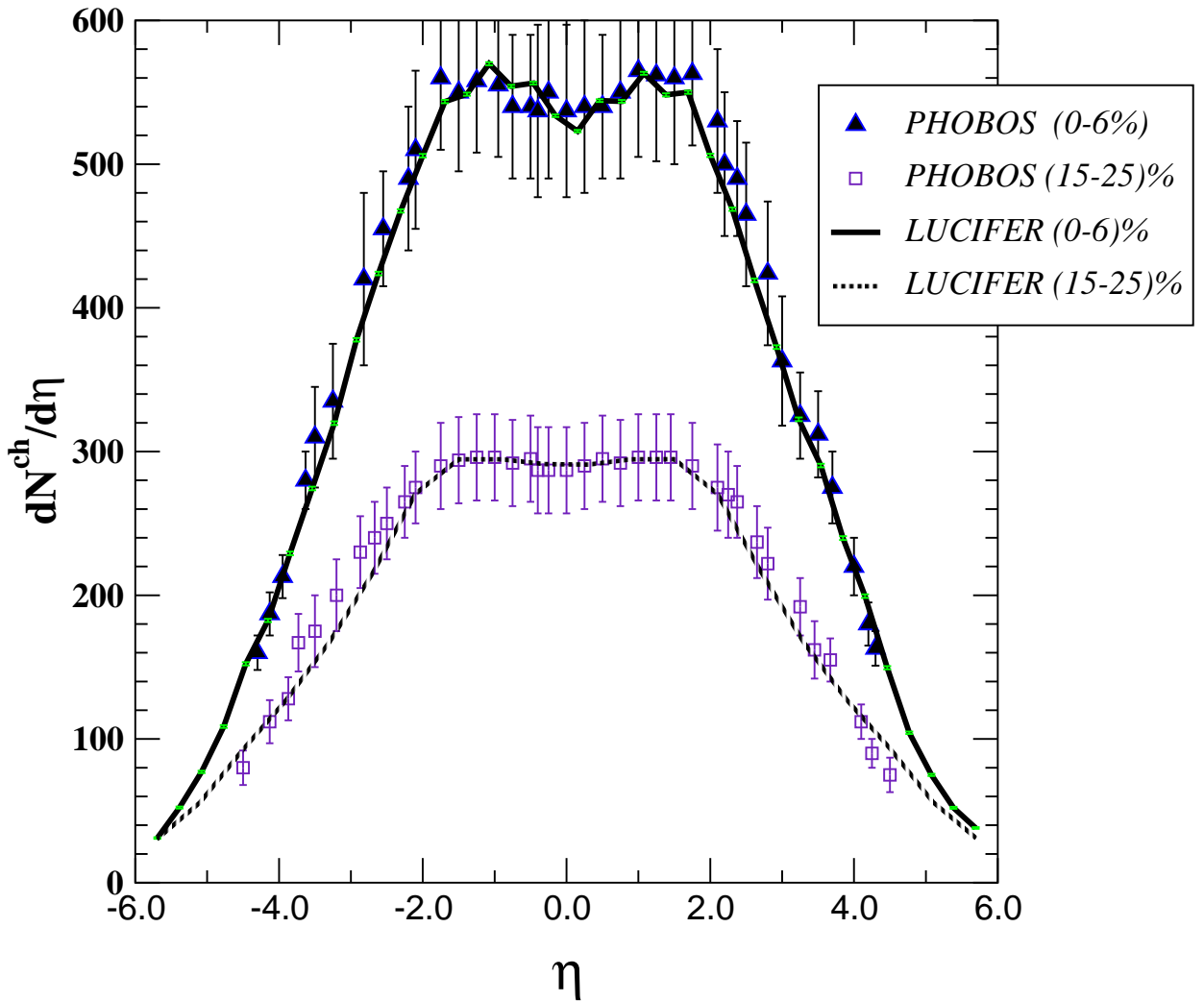


FIG. 5. Full pseudo-rapidity distributions for a representative selection of centrality cuts at $\sqrt{s} = 130$. The calculation for centrality of 20–25% has been normalised upward by $\sim 10\%$, consistent with the theoretical-experimental centrality dependence shown in Figure 3.

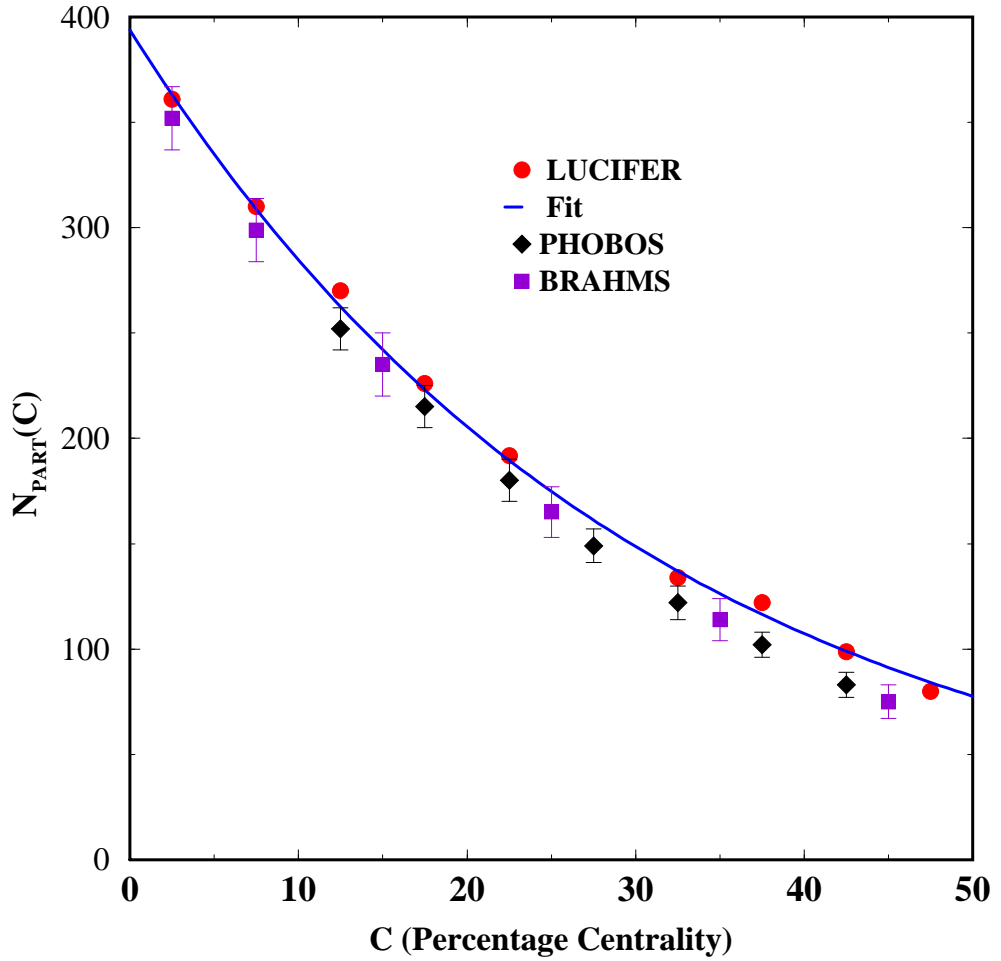


FIG. 6. Participant numbers from LUCIFER against those from BRAHMS and PHOBOS as a function of centrality. A fit to the simulation in the form $N^{part} = 394 \exp\{-.03355C\}$ is also displayed.

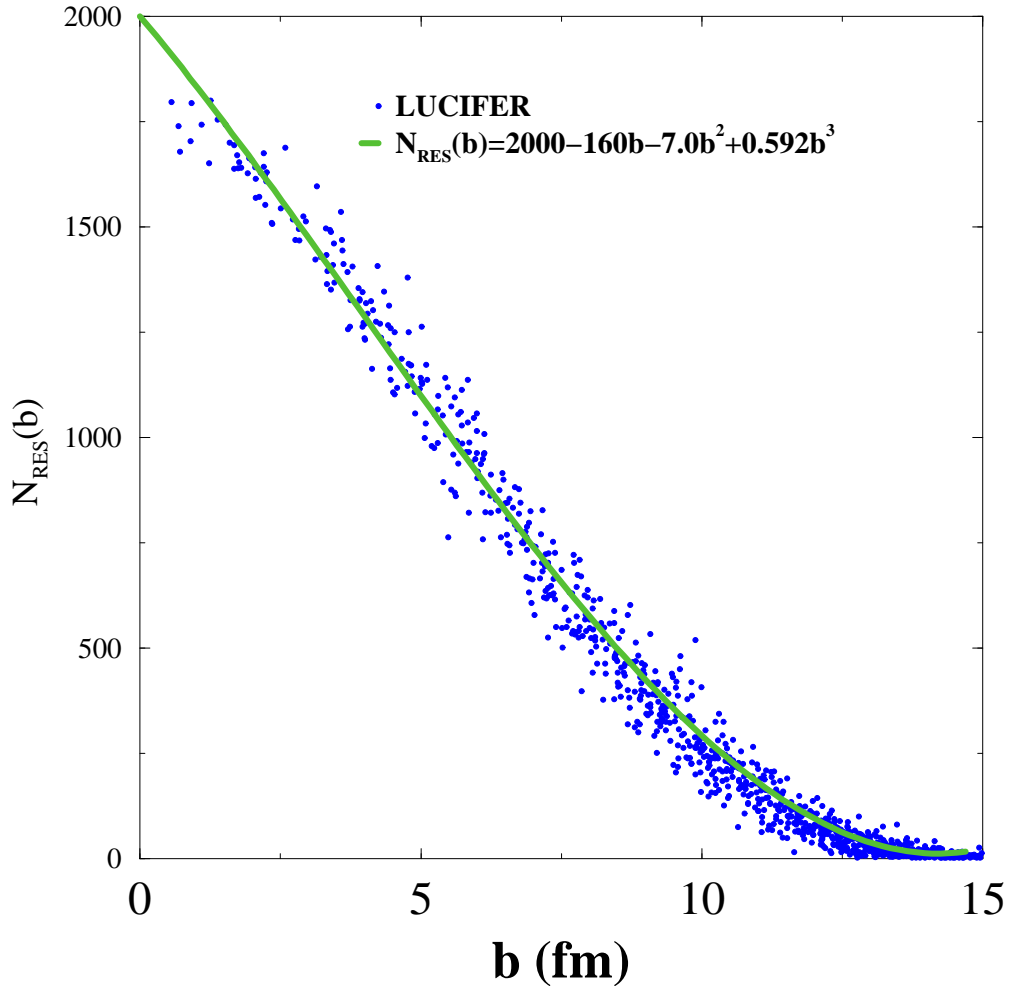


FIG. 7. The calculated distribution of generic bosonic resonances with impact parameter at the end of Phase I. These resonances are generated in Phase I and scatter and decay in Phase II. The particle and energy densities resulting from this distribution are discussed in the text.

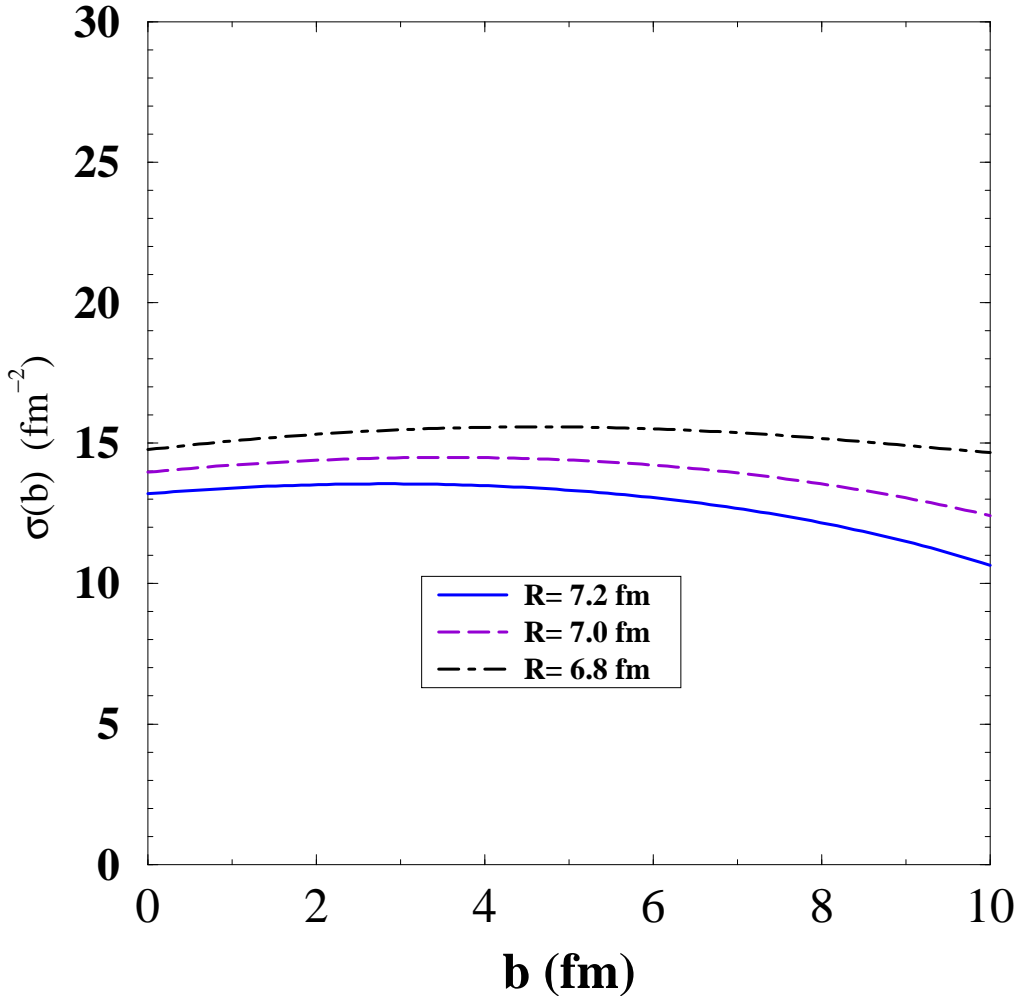


FIG. 8. The transverse areal density $\sigma_a(b, s)$ of generic resonances as function of impact parameter at three, radii R for colliding Au nuclei, assumed to be sharp spheres. The most evident feature is the slow variation of this density σ_a with b . For the largest R there is a residual $\sim 12\%$ drop in σ_a from $b = 5$ to $b = 10$ fm.

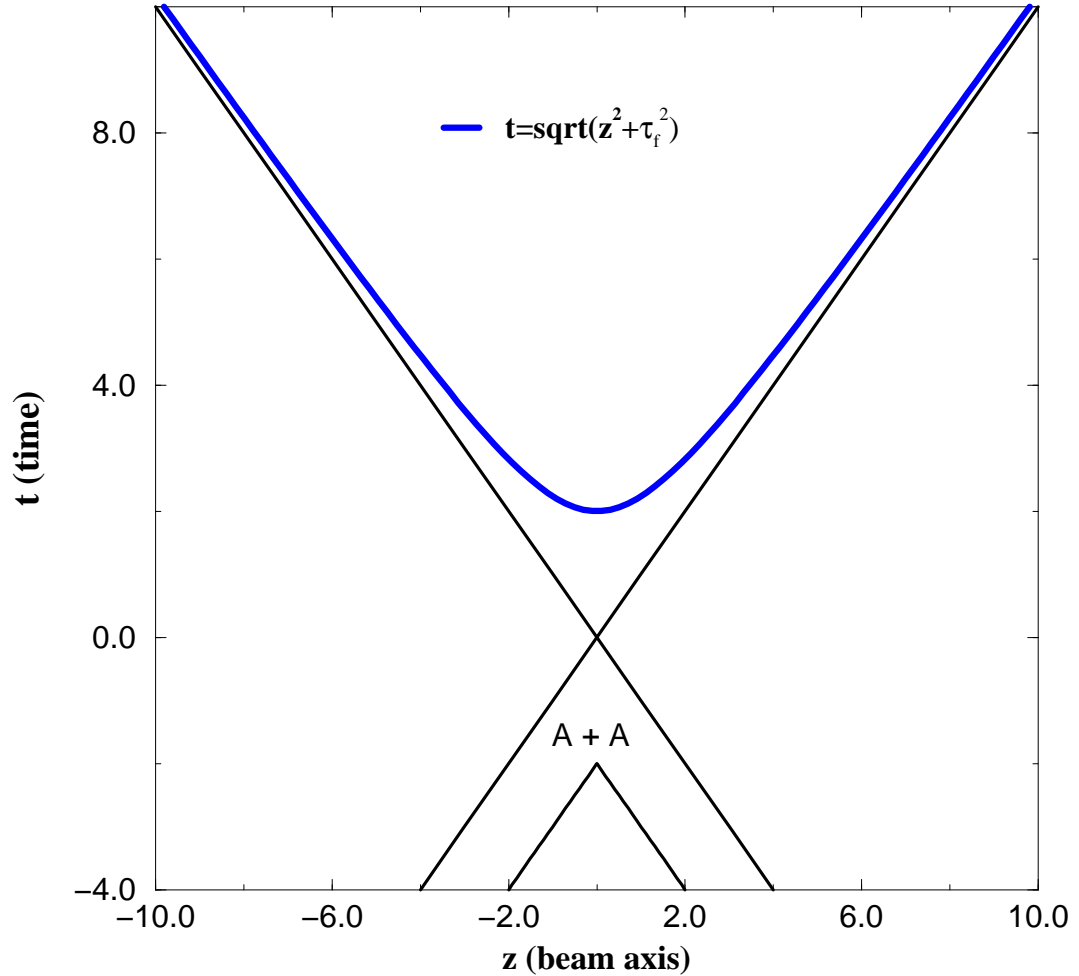


FIG. 9. A graphical space-time representation of the ion-ion collision. The second phase of the cascade begins along the solid upper curve shown in the figure. This curve is defined by the formation time τ_f , before which the generic bosonic resonances are not in play. Only longitudinal motion, along the beam axis, is represented.

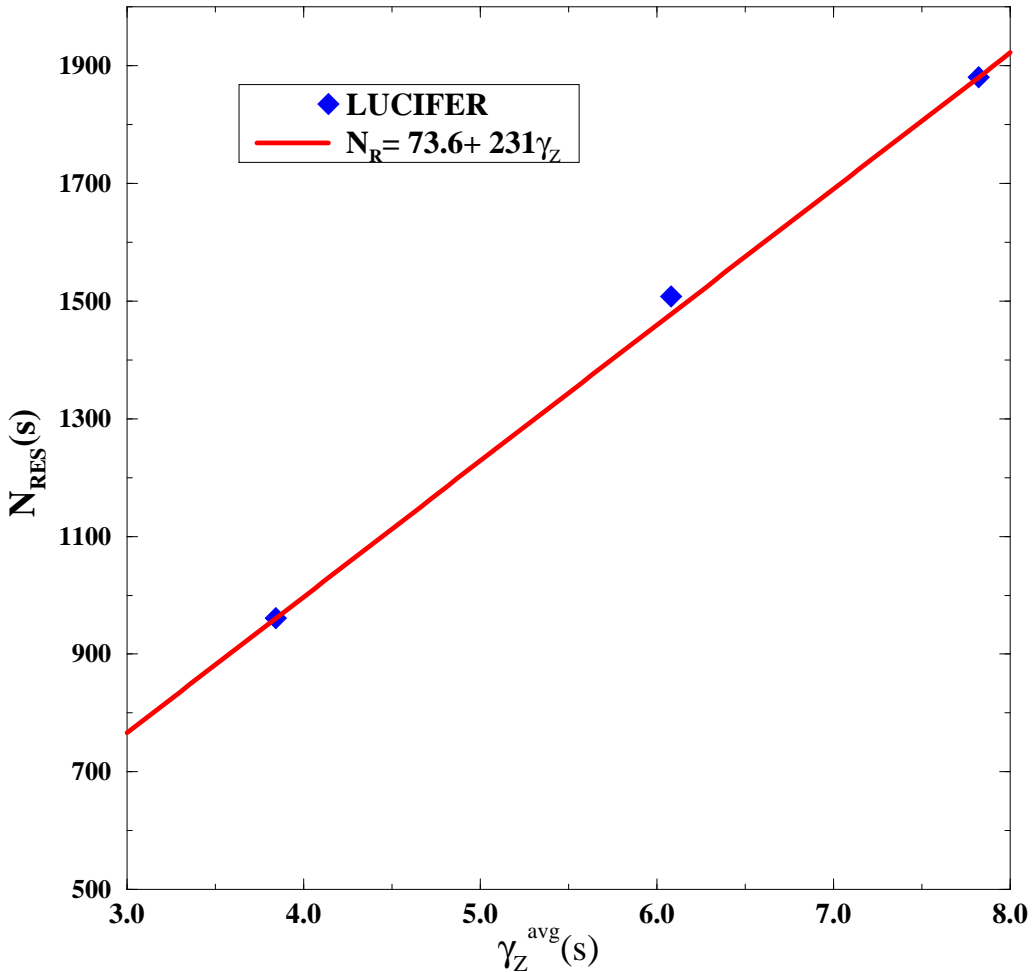


FIG. 10. Dependence of calculated $N_{\text{RES}}(s)$ on $\gamma_z(s)$ for $\sqrt{s} = 56, 130, 200$ GeV. The close to linear relationship between these variables defines the variation in final meson multiplicity with energy. The growth with s derives from the input KNO scaling and leads to a near constant, or saturated, spatial density.

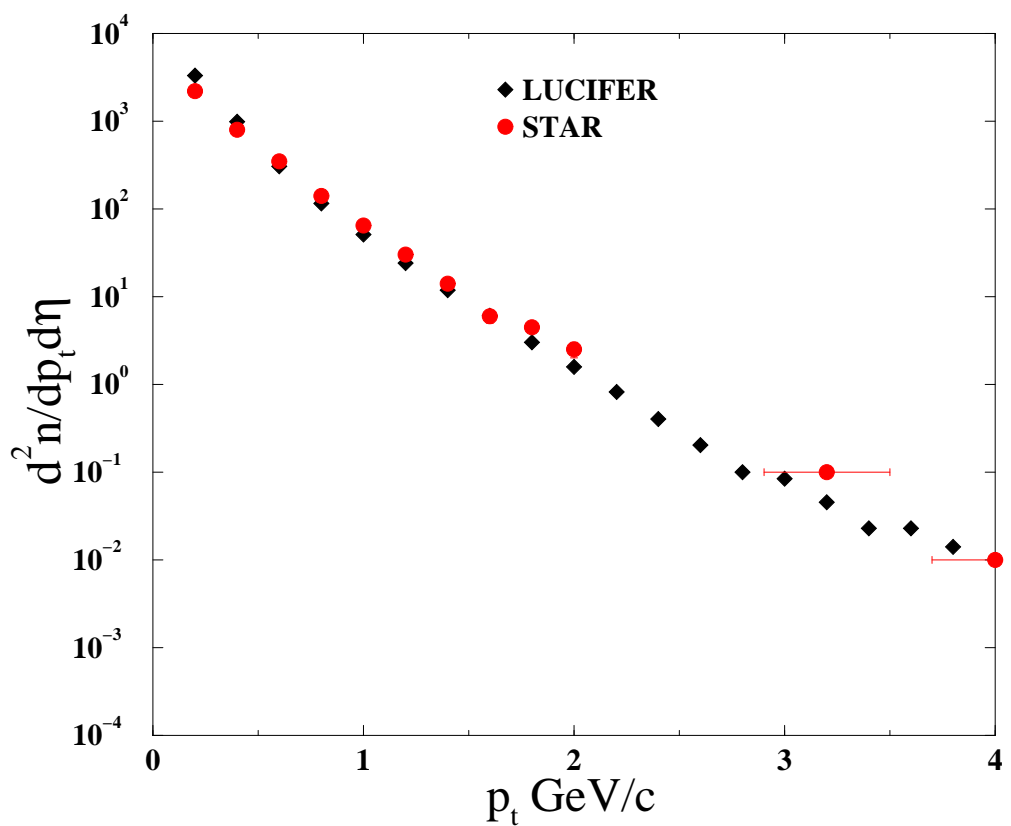


FIG. 11. Transverse momentum distribution. LUCIFER vs STAR. The experimental data includes all negative hadrons; for the theory anti-protons are omitted, but if included [7] they would make the agreement even closer for $p_t > 2$ GeV/c where \bar{p} becomes appreciable.